

Available online at scholarcommons.usf.edu/ijs

# International Journal of Speleology Official Journal of Union Internationale de Spéléologie



## Cryogenic ridges: a new speleothem type

Bogdan P. Onac 1,2, Daniel M. Cleary 1, Oana A. Dumitru 1,3, Victor J. Polyak 1,4 Ioan Povară<sup>5†</sup>, Jonathan G. Wynn 6, and Yemane Asmerom 64

<sup>1</sup>Karst Research Group, School of Geosciences, University of South Florida, 4202 E. Fowler Ave., NES 107, Tampa, 33620, USA

#### Abstract:

Cryogenic cave carbonates have been described from several formerly or presently glaciated karst caves. In most of these occurrences, they precipitated as loose grains or aggregates with various morphologies and sizes. Here, we report on a new speleothem type (cryogenic ridges) identified in Sohodoalele Mici Cave (SW Romania) within a large chamber near the entrance shaft. This study was motivated by the presence of a network of calcite ridges over the stalactites' surface and by the observation that during winter, these speleothems are covered by a thin ice layer. The higher  $\delta^{18}O$  (-3.5 to -1%) and  $\delta^{13}C$  (0 to 7%) values found in the calcite ridges relative to  $\delta^{18}O$  (-7.5 to -4%) and  $\delta^{13}C$  (-9 to -2%) values of calcite from the inner stalactite indicate that the ridges are of cryogenic origin and formed during relatively rapid carbonate precipitation associated with evaporative cooling and freezing of the water. Four U-series ages suggest that the stalactites with ridges formed during cold winters of the Holocene, when cave air temperatures dropped below freezing.

Keywords: freezing, cave, carbonate, stable isotopes, Romania

Received 18 February 2022; Revised 1 January 2023; Accepted 5 January 2023

Citation: Onac, B.P., Cleary, D.M., Dumitru, O.A., Polyak, V.J., Povară, I., Wynn, J.G., Asmerom, Y.,

2023. Cryogenic ridges: a new speleothem type. International Journal of Speleology, 52(1), 1-8.

https://doi.org/10.5038/1827-806X.52.1.2416

#### INTRODUCTION

Salts and ice coexist in various natural environments, including oceans, coastal regions, polar ice caps, and caves. Ice is highly intolerant to impurities. During freezing, dissolved ions in aqueous solutions are segregated and concentrated in the remaining, unfrozen liquid phase, from where they are ultimately precipitated as various cryogenic minerals (Hobbs, 2010). In karst regions, where groundwater chemistry is dominated by Ca2+ and HCO3-, or SO42- if gypsum strata are present, the most common cryogenic minerals are calcite and gypsum. In previously glaciated caves or those with perennial ice deposits, the most common cryogenic cave carbonates (CCC) appear to be calcite, aragonite, and ikaite (for a review see Žák et al., 2018). Although highly diverse morphologically, all cryogenic cave minerals have one common feature: they occur as loose crystals or aggregates. Ultimately, this can result in CCC accumulations of various thicknesses (1 to 50 mm) on the surface of the ice, within ice deposits, or on previous iced sections of cave floors. Summarizing a large number of publications, Žák et al. (2018) describe two types of cryogenic cave carbonates,  $\mathsf{CCC}_{\mathsf{fine}}$  and  $\mathsf{CCC}_{\mathsf{coarse}}$  that are defined by contrasting morphology and particle size (fine-grained powders vs. coarse crystals and aggregates), as well as isotopic signatures of carbon ( $\delta^{13}$ C) and oxygen ( $\delta^{18}$ O) (Clark & Lauriol, 1992; Žák et al., 2008). The  $CCC_{fine}$  are characterized by relatively high  $\delta^{18}O$  and  $\delta^{13}C$  values, with the latter reaching some of the highest measured values in freshwater carbonates (up to +17‰). They form due to rapid freezing of bicarbonate solutions, resulting in large kinetic fractionation. In contrast,  $CCC_{coarse}$  precipitate much slower than the  $CCC_{fine}$ , under cave settings that limit water evaporation and CO2 degassing. Depending on whether the system is open or closed with respect to CO<sub>2</sub> escape, the  $\delta^{13}$ C values may vary over a wide range (-10 to +7‰), whereas the  $\delta^{18}$ O values of the precipitated carbonates decrease (-10 to -25%) as the heavier <sup>18</sup>O is preferentially incorporated in the ice (Žák et al., 2004).

At present, CCC are widely recognized as speleothems that occur over different latitudinal and altitudinal ranges in caves hosting perennial ice, and in caves that are presently ice-free, but were glaciated

<sup>&</sup>lt;sup>2</sup>Emil Racoviță Institute, Babeș-Bolyai University, Clinicilor 5-7, 400006 Cluj-Napoca, Romania

<sup>&</sup>lt;sup>3</sup>Biology and Paleo Environment Department, Lamont-Doherty Earth Observatory, Columbia University, 61 Route 9W, Palisades, NY 10964, USA

Department of Earth and Planetary Sciences, University of New Mexico, 221 Yale Blvd. NE, Albuquerque, NM 87131, USA

<sup>&</sup>lt;sup>5</sup>Emil Racoviță Institute of Speleology, Romanian Academy, Frumoasă 31, 010986 Bucharest, Romania (†Deceased June 2022)

<sup>&</sup>lt;sup>6</sup>Division of Earth Sciences, National Science Foundation, 2415 Eisenhower Ave, Alexandria, VA 22314, USA

in the past. These two main occurrences of CCC have been identified in many caves in the Carpathians (Žák et al., 2004; Žák et al., 2008), Rhenish Massif (Richter & Riechelmann, 2008), Alps (Spötl, 2008; Colucci et al., 2017), Ural Mountains (Maximovitch & Panarina, 1966; Dublyansky et al., 2014, 2018; Mavlyudov & Kadebskaya, 2018), Canada (Clark & Lauriol, 1992; Lacelle et al., 2009), Rocky Mountains (Munroe et al., 2021), and lava tubes from Hawaii (Teehera et al., 2018). Most of these studies focus on mineralogy and morphology, but over the past decade, researchers have paired the occurrence of  $CCC_{\text{coarse}}$  with the particular cave climate condition under which they formed as a proxy for Late Pleistocene and Holocene climate changes (Lacelle, 2007; Richter et al., 2010; Žák et al., 2012; Luetscher et al., 2013; Dublyansky et al., 2014, 2018; Spötl et al., 2021).

Here, we use field observations, optical microscope imaging, and stable isotope analysis to characterize a new speleothem type, i.e., the cryogenic ridges, which is morphologically entirely different from all previously described CCC. We show that the stable isotope composition of calcite ridges crisscrossing the surface of stalactites provides clear evidence of their cryogenic origin, which is related to freeze-thaw processes occurring in a cave affected by strong seasonal air exchange.

#### Site and sample description

Sohodoalele Mici Cave is located in the Mehedinți Mountains of Southern Carpathians (SW Romania, Fig. 1a) and is carved in Lower Cretaceous limestones. It is a short cavity (210 m) that opens at 540 m above sea level (asl) at a bottom of a doline in a forested landscape (Bleahu et al., 1976). The cave is accessible by descending a 7 m deep shaft, at the bottom of which an ascending gallery extends east, but the main sections of the cave, including the Chamber with Stalactites à Facettes are oriented westward (Fig. 1b). There is a 10-m deep and narrow pit in the westernmost part of the cave that supposedly connects Sohodoalele Mici with Lazului Cave.

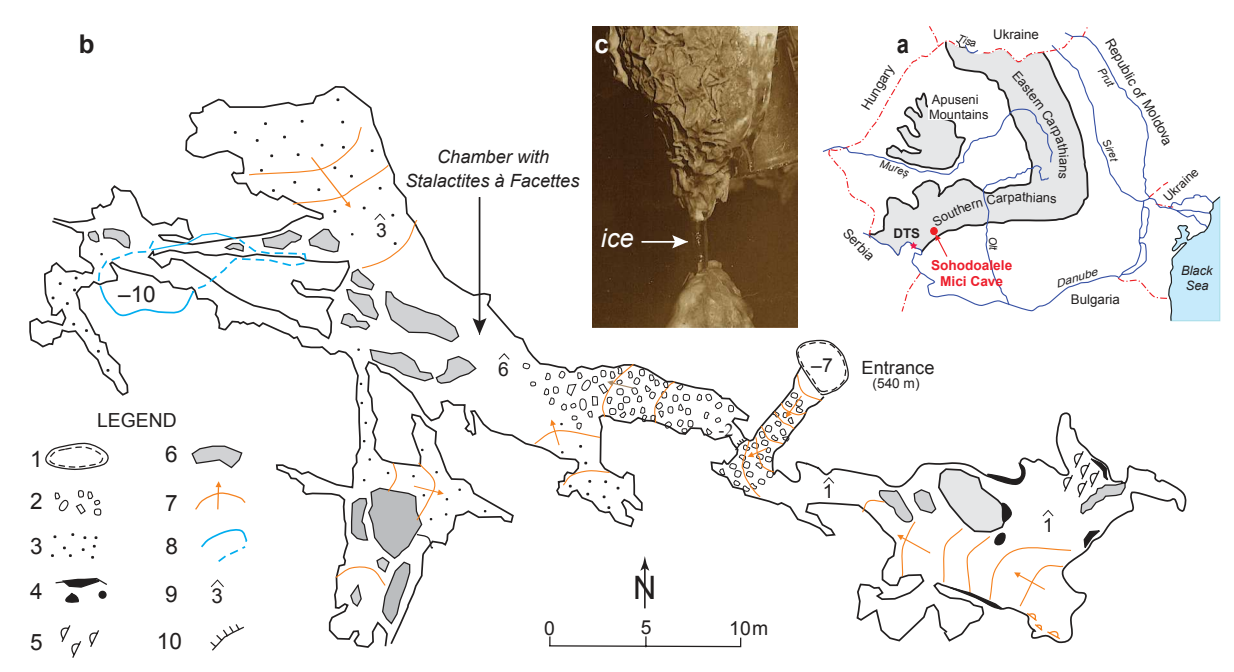


Fig. 1. a) Location of the Sohodoalele Mici Cave in SW Romania. DTS = Drobeta Turnu Severin Meteorological Station; b) Map of the cave showing the location of stalactites with cryogenic ridges. Legend: 1. Shaft; 2. Breakdown; 3. Sand; 4. Flowstone; 5. Pools; 6. Pillar; 7. Contour lines; 8. Lower level; 9. Height of the passage/room; 10. Cliff; c) Stalactite with cryogenic ridges and the corresponding stalagmite covered in ice (photo: I. Povară).

According to the Köpper climate classification, the Romanian Carpathians region has a wet temperate continental climate with two seasons: hot summers and long cold winters. In the Mehedinti Mountains, the climate is overall milder due to the sub-Mediterranean influences. The mean annual temperature (continuous 56 years record) at the nearest meteorological station (DTS in Fig. 1a) is 12.05°C, but the station is at a lower elevation (104 m asl) than the cave. Occasional measurements of the cave air temperature in the Chamber with Stalactites à Facettes indicate values between -2.3 and 3.7°C during winter months and as high as 8°C at the peak of the summer season. Due to the sub-vertical morphology of the cave, its ventilation is likely governed by the chimney effect, with an effective airflow during winter when cold and dense air sinks through the entrance shaft and

pushes the warm air out. This process is responsible for cooling enough the interior of the Sohodoalele Mici Cave to freeze dripping water (Fig. 1c). Nevertheless, the cave does not host perennial ice deposits because during the summer season, when airflow may occur along fractures and other flow paths inaccessible to humans, the cave air temperature is always above the freezing point of water.

Stalactites with a particular morphology (Fig. 2a-c), showing a network of ridges on their surface were first observed by V. Decu who named them "stalactites with facets" (a word-by-word translation from the French stalactites à facettes; Decu & Bleahu, 1967). The authors did not provide an explanation for their origin. This unusual speleothem was further investigated by Povară and Diaconu (1974) who noticed that ice covers them during winter (Fig. 1c). The genetic mechanism

proposed by the authors was that frost shattering is responsible for causing stalactites to crack and subsequently, during summer/fall, the percolating water feeding them would precipitate these calcite ridges. Following good cave conservation practice, the work reported here uses the original specimens collected and described by Povara and Diaconu (1974).

The two stalactites with ridges analyzed in this study are 10 and 15.1 cm long and have a maximum width of 3.8 cm (Fig. 2). The calcite ridges primarily precipitated parallel to the growth axis of the

stalactites, although a few ridges occur perpendicular or at different angles to it (Fig. 2a-c). The thickness of the ridges ranges from 0.5 to 4 mm. When split longitudinally, these composite speleothems (stalactites with cryogenic ridges) reveal a network of fine fractures, easily distinguished when griding/polishing powder fills the shatter cracks (Fig. 2d, e). Most of these fractures have a corresponding ridge on the stalactites' surface; however, others are filled with calcite. The cryogenic ridges on some stalactites are covered by coralloids (Fig. 2e); their presence is addressed in the Discussion section.

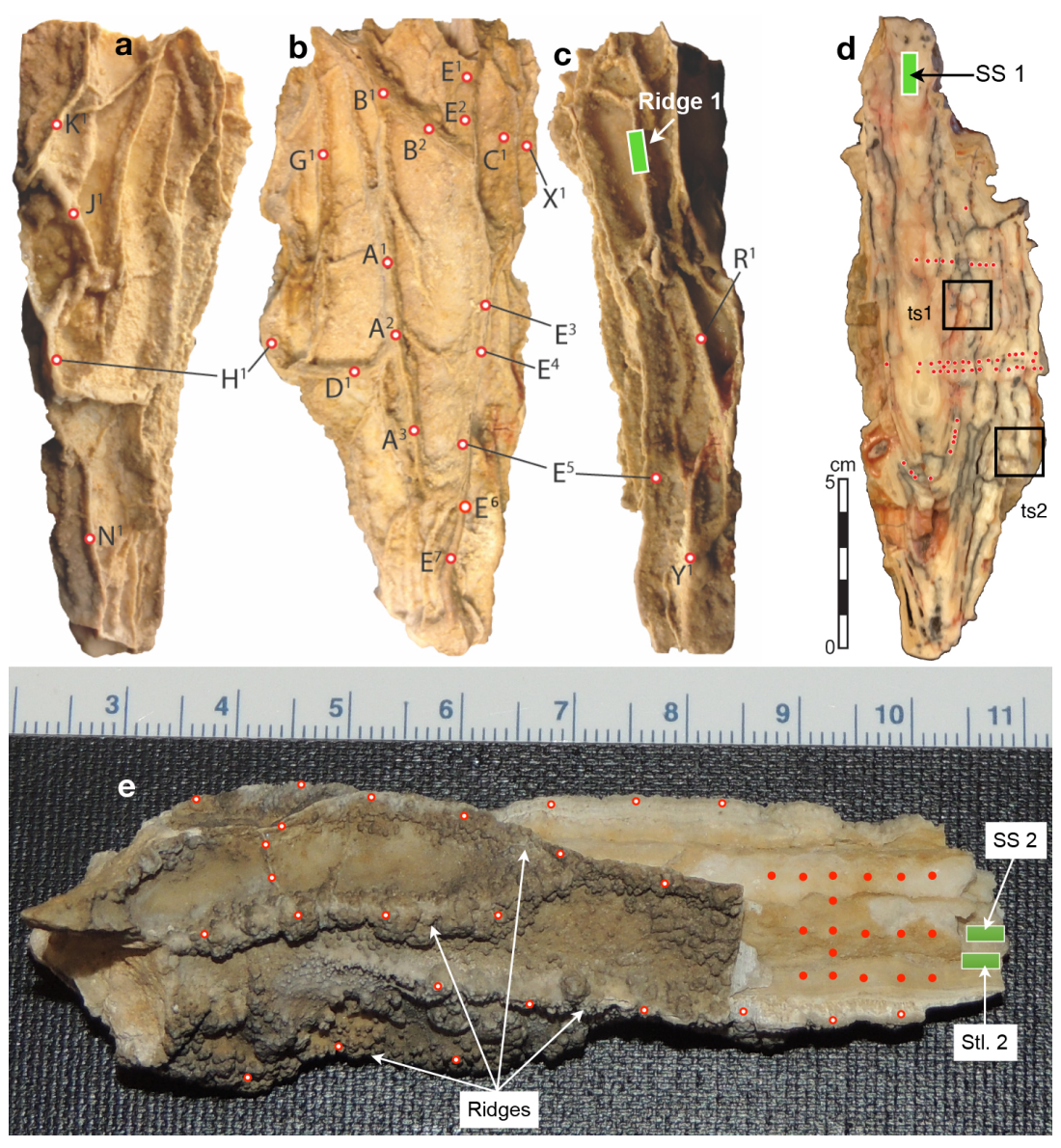


Fig. 2. Multiple perspectives of Stalactite 1 showing the network of calcite ridges and the location of samples (red/white circles) for stable isotope analysis. a) Left side profile; b) Front view; c) Right side profile showing Ridge 1 used for U-series dating (green rectangle). H1 (in a, b) and E5 (in b, c) are marked to help connecting perspectives of the stalactite; d) Cross-section view of the stalactite with the location of thin sections (black squares) and of common calcite sampled for stable isotope analyses (red dots); e) Stalactite 2 showing the position of analyzed samples (color codes as above).

#### **METHODS**

Hand specimens and thin sections were studied microscopically using a Keyence VHX-7000 digital microscope (magnification 10x to 5000x) equipped with a free-angle observation system (VHX-S770E) with a polarizer, and a custom-built lambda filter. Due to the fragility of the available samples, only two thin sections (ts1 and ts2) were manufactured from Stalactite 1 (Fig. 2d).

A total of 125 carbonate powders (80-120  $\mu$ g each) were drilled using a vertical Sherline micro-milling machine. Sampling was carefully done along and across different layers, along horizontal and vertical cross-sectional transects, around single growth layers, and across calcite ridges (see Fig. 2). All samples were analyzed for oxygen and carbon isotopic ratios in CO<sub>2</sub> obtained by reacting carbonate powders with H<sub>3</sub>PO<sub>4</sub> at 25°C for 24 hours. Carbon and oxygen isotope ratios

were measured on a Thermo Delta V Isotope Ratio Mass Spectrometer at the Stable Isotope Laboratory, School of Geosciences, the University of South Florida in Tampa (USA). The results are expressed in delta (δ) notation using the following formula:  $\delta = [(R_{sample}/R_{std})]$ – 1]·1000, reported in ‰, where  $R_{\text{sample}}$  is the ratio of  $^{13}\text{C}/^{12}\text{C}$  or  $^{18}\text{O}/^{16}\text{O}$  of carbonates and  $\dot{R}_{std}$  are the same ratios of the international reference standard Vienna PDB (VPDB). All sample  $\delta$ -values were normalized to the VPDB scale using two reference materials (NBS-18 and an in-house standard of Carrara Marble, NewCar), which were analyzed at the beginning of the sequence, after every five samples, and at the end of each batch of samples. For the two reference materials, the  $\delta^{13}$ C and  $\delta^{18}$ O values used were -5.04%and -23.05% for NBS-18 and +4.04 and 3.38% for NewCar; the latter was normalized to the values of +1.95% and -2.20% for the NBS-19 international reference material. Duplicate measurements of the reference materials show that the reproducibility for  $\delta^{13}C$  and for  $\delta^{18}O$  values is better than  $\pm~0.08\%$  and  $\pm$ 0.06‰ (1σ), respectively.

Four calcite subsamples (SS 1 and Ridge 1 on Stalactite 1, and SS 2 and Stl. 2 on Stalactite 2; green rectangles in Fig. 2) were dated using the U-series technique in the Radiogenic Isotope Laboratory of the University of New Mexico in Albuquerque (USA) to constrain the timing of both stalactites and their calcite blade growth. The aliquots were sampled from the most crystalline parts of the stalactites. Subsample powder sizes range from 85 to 205 mg. They were then etched with 3% HNO<sub>3</sub>, rinsed in 18 M $\Omega$ water, and dried at 150-180°C. Each mineral aliquot was weighted (50-150 mg), dissolved in 15N HNO<sub>3</sub>, and spiked with a 229Th-233U-236U mixed tracer. One to two drops of HClO<sub>4</sub> were added for spike-sample equilibration and to eliminate organic contaminants. The solution was fluxed for ~1-2 hours and dried down. Uranium (U) and thorium (Th) were separated using Eichrom 1x8 chloride form 200-400 mesh anion resins. U and Th were eluted using 6N HCl

and H<sub>2</sub>O, respectively, and the solutions were dried down and dissolved in 0.5N HNO<sub>3</sub> for analysis. The isotopes of U and Th were measured in separate runs using a Thermo Neptune multi-collector inductively coupled plasma mass spectrometer (Asmerom et al., 2006). The U-series ages were calculated using the decay constants reported in Cheng et al. (2013).

#### RESULTS

The microscope images of the longitudinally polished surface of the halved Stalactite 1 show fractures running lengthwise and across the speleothem. Some of these cracks are filled with calcite or polishing black powder, whereas others are open (Fig. 2d and Supplementary Fig. S1a, b). Thin section examination reveals the existence of open and calcite-filled fractures that cut across well-developed columnar calcite crystals (Supplementary Fig. S1c, d). The cryogenic ridges protruding on the surface of stalactites are continuous (up to 10 cm in length) or fragmented (zigzagging), and their outermost part is either open (resembling a micro-rift; Supplementary Fig. S2a, c-d) or appears as parallel furrows (Supplementary Fig. S2b).

The isotopic analysis identifies two groups of data that plot on distinct fields, each of them being relatively homogeneous. Population 1 (red symbols in Fig. 3) represents powders from the common calcite stalactite and have values between -8 and -2% and between -6.5 and -3.9% for  $\delta^{13}$ C and  $\delta^{18}$ O, respectively. In contrast, the calcite samples from various ridges (Population 2, blue symbols in Figure 3) have higher values for both  $\delta^{18}$ O (-3.5 to -1%) and  $\delta^{13}$ C (0 to 7%).

All calcite samples selected for U-series dating show low uranium concentrations and large amounts of <sup>232</sup>Th (Table 1). The initial <sup>230</sup>Th corrections associated with the high detrital Th led to large ages uncertainties. Nevertheless, the age data show that the two stalactites formed during the Holocene. Only one age (Ridge 1) was obtained on calcite ridges because of their small size and overall high detrital Th.

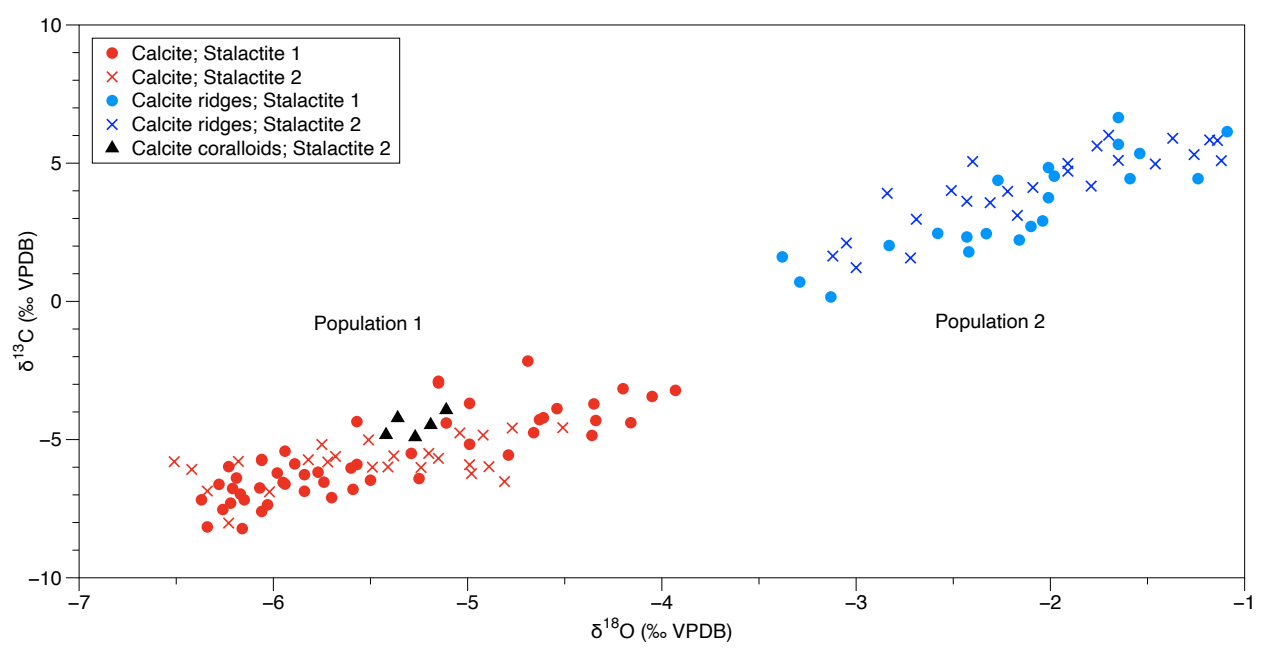


Fig. 3. Oxygen and carbon isotope values of common calcite in stalactites and calcite ridges from Sohodoalele Mici Cave.

Table 1. U-series dating results. All uncertainties are absolute  $\pm 2\sigma$ . Initial  $^{230}$ Th/ $^{232}$ Th atomic ratio used to correct ages is  $4.4 \pm 50\%$ . yrs BP = years before present, where present = AD 2021.

Sample	<sup>238</sup> U (ppb)	<sup>232</sup> Th (ppt)	<sup>230</sup> Th/ <sup>232</sup> Th activity	<sup>230</sup> Th/ <sup>238</sup> U activity	Measured δ <sup>234</sup> U (‰)	Initial δ <sup>234</sup> U (‰)	Uncorr. age (yrs BP)	Corrected age (yrs BP)
SS 1	433.02±0.35	98,459±125	2.32±0.02	0.172±0.001	559±2	573±4	12,692±101	8,410±2,124
Ridge 1	32.08±0.03	1,449±46	7.19±0.34	0.106±0.004	690±2	702±2	7,055±256	6,280±464
SS 2	116.1±0.09	14,746±26	1.76±0.02	0.073±0.001	1147±2	1154±4	3,758±46	2,031±862
Stl. 2	191.76±0.11	21,136±24	1.63±0.02	0.059±0.001	1162±2	1166±3	3,003±32	1,514±743

#### **DISCUSSION**

The separation of the isotopic data in two fields (Fig. 3) suggests that different processes are responsible for the formation of common speleothems and their calcite ridges. Clark and Lauriol (1992) and Žák et al. (2004; 2008) pioneered the study and the recognition of cryogenic carbonate speleothems by using their micro-morphology and stable isotopic composition. The vast majority of the common calcite samples from the Sohodoalele Mici Cave have  $\delta^{18}O$ and  $\delta^{13}$ C values that fall within the normal range of secondary calcite in karst caves (Fig. 4, dashed rectangle). This suggests that the stalactites did not form under freezing conditions, but as a result of CO<sub>2</sub> outgassing as drip water enters the cave, which led to supersaturation and calcite precipitation (Fairchild & Baker, 2012; Hansen et al., 2013). This inference is supported by the presence of the original soda straw, a speleothem with a morphology not associated with cryogenic processes. Alternatively, the higher  $\delta^{18}O$  and  $\delta^{13}C$  values in the associated calcite ridges are consistent with a process that involves freezing of calcium bicarbonate-rich drip water. Yet, the stalactites with ridges are entirely different from the morphology of carbonate aggregates/powders or cave pearls that were previously recognized as typical of fine or coarse CCC (Žák et al., 2018). To determine the type of freezing process that generated the ridges, their isotopic values are plotted alongside those of other reported cryogenic carbonates (Fig. 4). The high  $\delta^{\scriptscriptstyle 13} C$  and  $\delta^{\scriptscriptstyle 18} O$  values in the calcite ridges fall within a range similar to that of  $CCC_{\text{fine}}$  described by Žák et al. (2008, 2009) and Munroe et al. (2021). This suggests that the calcite ridges from the Sohodoalele Mici Cave originate from rapid freezing of water accompanied by fast calcite precipitation (Žák et al., 2018), unlike the CCC documented from Cold Winter and Winter Wonderland caves of the Western US (blue circles and purple triangles in Fig. 4) which formed through slow freezing of water. Since the present study focuses solely on stalactites with ridges, samples from the cave floor, where fine and coarse CCC could exist, were not collected.

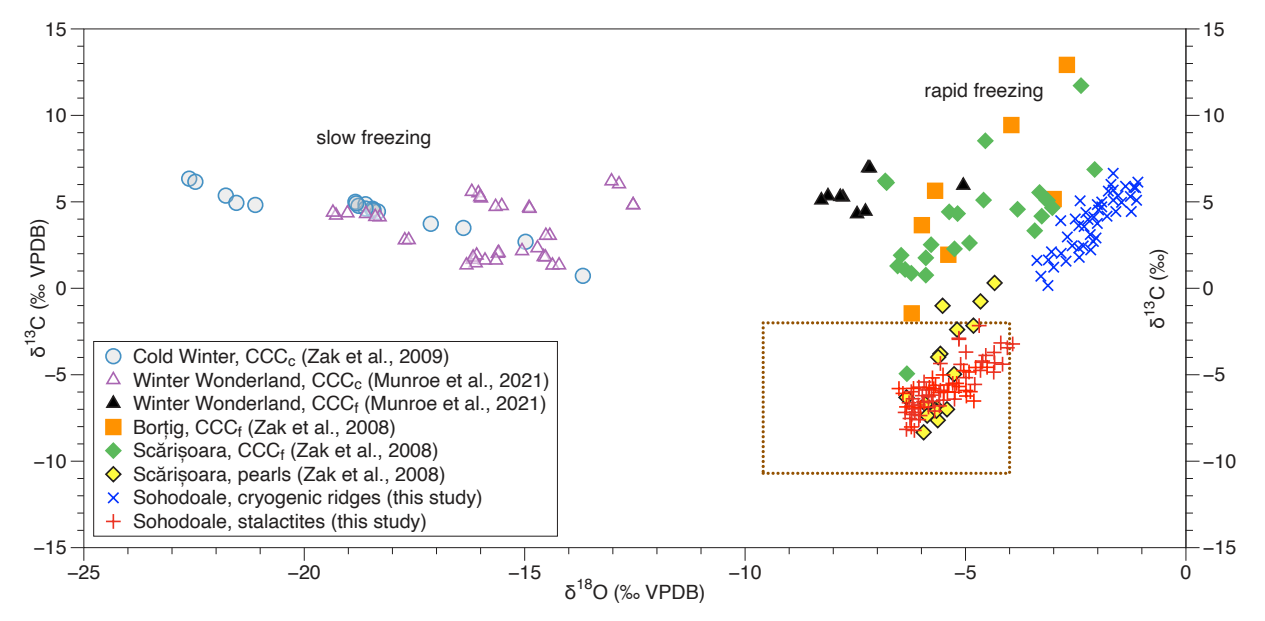


Fig. 4. Isotopic data of cryogenic and non-cryogenic carbonates from Sohodoalele Mici Cave and different other caves in Central and East-Central Europe and the USA. The dashed rectangle marks the isotopic range of common speleothems from non-iced caves.

Both stalactites are small, and it is likely that the growth history of each covers hundreds, rather than thousands, of years. Unfortunately, due to the large uncertainties in the U-series ages, the timing of their formation is poorly constrained. Nonetheless, the results show that SS 1 and Ridge 1 precipitated in the Early to Middle Holocene and SS 2 in the Late Holocene. The stable isotopic data alone (Fig. 3) cannot clarify whether the two isotopically different

populations of calcite ridges and common stalactites formed synchronously or at different times. However, the relationship between the calcite ridges and the inner structure of their host stalactites is clear, especially when inspected in longitudinal cut (Fig. 1d and Supplementary Fig. S1). All ridges appear to have precipitated at the edge (outer part) of a network of fissures (black lines in Fig. 2d) after or during a late stage in the stalactite growth. Based on the cross-

cutting relationship of the ridges and the surface of the stalactite (Supplementary Fig. S2), we hypothesize that the former is younger. SS 2 started forming at ~2,900 years ago (i.e., adding the age uncertainty of 862 yrs to 2,031 yrs BP), and the outer layers of the stalactite (Stl. 2) formed within the last 2,250 years (i.e., 1,514  $\pm$  743 yrs BP). This shows that the maximum time for the ridges to develop is less than ~2,250 years, and probably significantly less. Precipitation of Ridge 1 took place ~6,280  $\pm$  464 yrs BP, and it is likely that the growth period was a few millennia at most since the SS 1 begun its growth ~10,500 years ago (8,410  $\pm$  2,124 yrs BP).

#### The mechanism for forming cryogenic ridges

As shown above, the cryogenic ridges are younger than most stalactite growth. The formation of stalactites occur under vadose conditions during warm periods when the cave air temperature is above freezing. The visual inspection of the inner part of the two ridged stalactites reveals the presence of soda straws (Fig 5a), which evolved into conical stalactites as percolating water flows down the outer part of the straws (Fig. 5b). The constant cave temperature, relative humidity close to 100%, and negligible evaporation, suggest the likelihood of near-equilibrium isotope fractionation during the speleothem deposition. This implies lower isotope effects during calcite precipitation, resulting in a narrower range of lower  $\delta^{13}C$  and  $\delta^{18}O$  values (Dreybrodt & Scholz, 2011), which contrasts the higher isotopic values of the cryogenic ridges (Fig. 4).

Even when the cave air temperature drops below freezing, warmer vadose percolating water continues to feed the speleothems. Freezing will block the flow through the soda straw and promote the development of a thin layer of ice over the stalactites (Fig. 1c) that can lead to cryofracturing near the stalactite surface (Fig. 5c). Any water present inside stalactites (i.e., pores or/and capillaries) will also freeze and expand (increase volume), generating a network of fine fissures inside the speleothem (Fig. 5c). During subsequent winter periods, the ice plugs the tip of the soda straw, thus forcing the flow of percolating water through the inner network of fissures (Fig. 5d). The water reaching the surface of the stalactite freezes causing CO2 to degas rapidly, triggering calcium carbonate precipitation as the water-ice front advances during the ice crystal growth (Fig. 5d and inset). This outgassing results in the oversaturation of the residual water and enables faster calcite deposition at the outer part of the fractures, thus building ridges. Towards the beginning of spring, the fractures seal up or water is directed through the soda straw tube rather than going through the capillary cracks. Once the ridges have formed, warmseason percolating waters that coat the stalactite and add new calcite layers are kept away from the higher ridges. The following year, the process repeats itself and the ridges continue to develop in this way during the growth of the stalactite. The observation that some of the cryogenic ridges are covered by irregular coralloids (Fig. 1e) indicates strong evaporation. Such conditions are also suggested by the higher  $\delta^{13}C$  and δ<sup>18</sup>O values (see black triangles in Figure 3). Following this scenario, common calcite precipitates during summer increasing the size of the stalactite, whereas cryogenic calcite ridges only form during cold seasons. With this proposed process, the ridges develop during stalactite growth, but only after soda straws become conical stalactites.

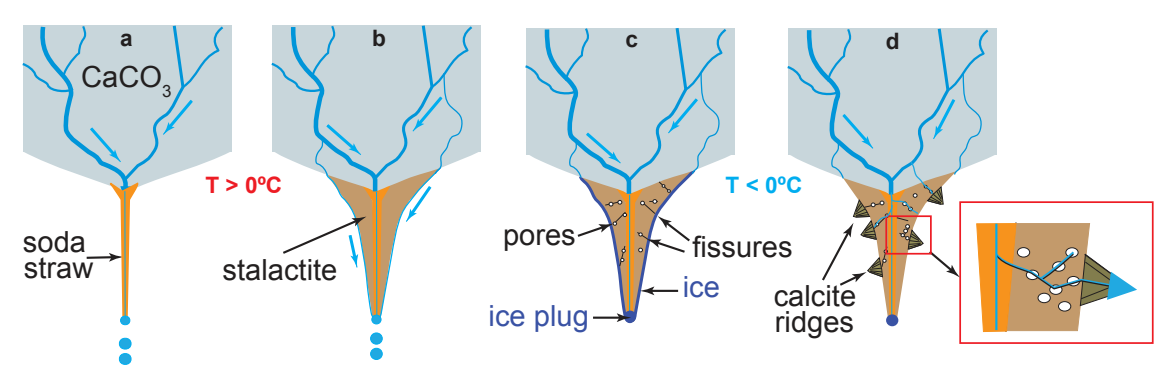


Fig. 5. Schematic illustration showing the phases that lead to the formation of stalactites with ridges. a) Precipitation of calcite soda straw; b) Development of conical stalactites as water flows down their outer surfaces; c) Ice covers stalactites and minor fissures occur due to freezing both at the surface and within the stalactites; d) Percolating water seeps out the capillary fissures during the winter freezing periods leading to the accretion of cryogenic calcite that forms ridges.

During the deposition of cryogenic calcite ridges, the carbon and oxygen stable isotope composition is controlled mainly by kinetic isotopic effects that under open-system conditions shift the  $\delta^{18}O$  and  $\delta^{13}C$  towards higher values. This is because evaporative cooling (dry air moving over moist surface) or/and freezing of water (due to latent heat loss) lead to  $^{18}O$ -enriched residual water out of which the cryogenic carbonates precipitated. The winter-season dynamic cave airflow promotes rapid freezing and fast calcite precipitation. During the latter process,  $^{12}C$  is released into the cave air as  $CO_2$  causing the residual fraction of bicarbonate

in the water (before complete freezing) to be  $^{13}$ C-enriched and therefore, the  $\delta^{13}$ C in the newly forming cryogenic carbonate progressively shifts towards higher values.

The above results suggest that gelifraction (freeze-thaw fracturing) is the mechanism responsible for the particular morphology of the speleothems in the Chamber with Stalactites à Facettes. This process was first suggested by Povară and Diaconu (1974) after they noticed ice-covered stalactites in Sohodoalele Mici Cave, but lacked additional evidence to support their theory. The new data reported here, not only confirm the hypothesized genetic mechanism, but also allow

the classification of a new speleothem type, which according to Hill and Forti (1995, 1997), represents "a group or category of speleothems sharing one or more morphological characteristics and having a common origin different from other speleothem types". In this case, the network of cryogenic ridges occurring at the surface of stalactites represents the new speleothem type. The stalactites with ridges are therefore a composite speleothem with an atypical morphology produced by freezing, which is additional to the hydrologic mechanism (dripping/flowing) that forms common stalactites. It is worth noting that in the period of writing this paper, cryogenic ridges were observed by one of the authors (BPO) in the Demänovská Ice Cave (Slovakia), where they occur both on stalactites (Supplementary Fig. S3) and calcite crusts covering cave walls.

#### **CONCLUSIONS**

This study represents the first recognition of a new speleothem type, named cryogenic ridge that contributes to the growth and final morphology of a composite speleothem called stalactite with ridges. The contrasting isotopic composition of calcite in common stalactites and ridges further emphasize their different genetic mechanisms. The evaporative cooling and freezing of water cause the residual solutions to become supersaturated and enriched in <sup>18</sup>O; consequently, the cryogenic calcite ridges precipitated from them will have higher  $\delta^{18}$ O values. During rapid freezing and fast calcite precipitation, the preferential outgassing of 12C from water shifts the δ<sup>13</sup>C values of the residual solution to progressively higher values, which are then found in the calcite that forms the ridges. In contrast, the lower values in the non-ridged calcite fall within the typical range for common carbonate speleothems. This finding suggests that apart from the typical fine or coarse CCC, freezing may be responsible as whole or in part for the precipitation of other cryogenic speleothems.

#### **ACKNOWLEDGEMENTS**

Carolyn Lang is thanked for helping with the preparation of stable isotope samples, and Jessica Wilson for support of the analysis at the USF-Tampa Geosciences Stable Isotope Laboratory. JGW was supported by an NSF IR/D program. Authors acknowledge the discussions with Carol A. Hill, Paolo Forti, and Jo De Waele on the speleothem terminology. We thank Drs. A. Germa and S. Charbonnier for access to the Keyence VHX-7000 microscope, acquired through NSF grant EAR-204006.

**Authorship statement:** BPO and IP designed the research. DMC, OAD, JGW, and BPO collected and performed the isotope analysis. VJP and YA measured U-series ages of speleothems. BPO drafted and wrote most of the manuscript with input from all authors.

#### REFERENCES

Asmerom, Y., Polyak, V., Schwieters, J., Bouman, C., 2006. Routine high-precision U–Th isotope analyses for

paleoclimate chronology. Geochimica et Cosmochimica Acta, 70(18), A24.

https://doi.org/10.1016/j.gca.2006.06.061

Bleahu, M., Decu, V., Negrea, Ş., Pleşa, C., Povară, I., Viehmann, I., 1976. Peşteri din România. Editura Ştiințifică şi Enciclopedică, Bucureşti, 416 p.

Cheng, H., Edwards, R.L., Shen, C.-C., Polyak, V.J., Asmerom, Y., et al., 2013. Improvements in <sup>230</sup>Th dating, <sup>230</sup>Th and <sup>234</sup>U half-life values, and U–Th isotopic measurements by multi-collector inductively coupled plasma mass spectrometry. Earth and Planetary Science Letters, 371, 82–91.

https://doi.org/10.1016/j.epsl.2013.04.006

Clark, I.D., Lauriol, B., 1992. Kinetic enrichment of stable isotopes in cryogenic calcites. Chemical Geology, 102(1), 217–228.

https://doi.org/10.1016/0009-2541(92)90157-Z

Colucci, R.R., Luetscher, M., Forte, E., Guglielmin, M., Lenaz, D., Princivalle, F., Vita, F., 2017. First alpine evidence of in situ coarse cryogenic cave carbonates (CCC<sub>coarse</sub>). Geografia Fisica e Dinamica Quaternaria, 40(5), 53–59.

Decu, V., Bleahu, M., 1967. Grottes d'Olténie explorées de 1959 à 1962. In: Decou, A., Decou, V., Bleahu, M. (Eds.), Recherches sur les grottes du Banat et d'Olténie (Roumanie, 1959–1962). Centre National de la Recherche Scientifique (CNRS) Éditions, Paris, p. 327–329.

Dreybrodt, W., Scholz, D., 2011. Climatic dependance of stable carbon and oxygen isotope signals recorded in speleothems: From soil water to speleothem calcite. Geochimica et Cosmochimica Acta, 75, 734-752. https://doi.org/10.1016/j.gca.2010.11.002

Dublyansky, Y., Kadebskaya, O., Luetscher, M., Cheng, H., Chaykovskiy, I., Spötl, C., 2014. Preliminary data on the Pleistocene history of the permafrost in Central Urals (Russia) derived from cryogenic cave carbonates, Proceedings of the Conference The Quaternary of the Urals Global Trends and Pan-European Quaternary records. INQUA-SEQS, Ekaterinburg, p. 43–44.

Dublyansky, Y., Moseley, G.E., Lyakhnitsky, Y., Cheng, H., Edwards, L.R., Scholz, D., Koltai, G., Spötl, C., 2018. Late Palaeolithic cave art and permafrost in the Southern Ural. Scientific Reports, 8(1), 12080. https://doi.org/10.1038/s41598-018-30049-w

Fairchild, I.J., Baker, A., 2012. Speleothem science: From process to past environments. Wiley-Blackwell, Chichester, 448 p.

https://doi.org/10.1002/9781444361094

Hansen, M., Dreybrodt, W., Scholz, D., 2013. Chemical evolution of dissolved inorganic carbon species flowing in thin water films and its implications for (rapid) degassing of CO<sub>2</sub> during speleothem growth. Geochimica et Cosmochimica Acta, 107, 242-251. <a href="https://doi.org/10.1016/j.gca.2013.01.006">https://doi.org/10.1016/j.gca.2013.01.006</a>

Hill, C.A., Forti, P., 1995. The classification of cave minerals and speleothems. International Journal of Speleology, 24(1-4), 77–82.

https://doi.org/10.5038/1827-806X.24.1.5

Hill, C.A., Forti, P., 1997. Cave minerals of the world (2nd ed). National Speleological Society, Huntsville, AL, 464 p.

Hobbs, P.V., 2010. Ice physics. Oxford University Press, Oxford, 856 p.

Lacelle, D., 2007. Environmental setting, (micro) morphologies and stable C-O isotope composition of cold climate carbonate precipitates - a review and evaluation of their potential as paleoclimatic proxies. Quaternary Science Reviews, 26(11–12), 1670–1689.

https://doi.org/10.1016/j.quascirev.2007.03.011

Lacelle, D., Lauriol, B., Clark, I.D., 2009. Formation of seasonal ice bodies and associated cryogenic carbonates in Caverne de l'Ours, Québec, Canada: kinetic isotope effects and pseudo-biogenic crystal structures. Journal of Cave and Karst Studies, 71(1), 48–62.

Luetscher, M., Borreguero, M., Moseley, G.E., Spötl, C., Edwards, R.L., 2013. Alpine permafrost thawing during the Medieval Warm Period identified from cryogenic cave carbonates. The Cryosphere, 7(4), 1073–1081. https://doi.org/10.5194/tc-7-1073-2013

Mavlyudov, B.R., Kadebskaya, O.I., 2018. Ice caves in Russia, In: Perşoiu, A., Lauritzen, S.E. (Eds.), Ice caves. Elsevier, Amsterdam, p. 529–610.

https://doi.org/10.1016/B978-0-12-811739-2.00026-7 Maximovitch, G.A., Panarina, G.N., 1966. Chemical composition of cave ice from the province of Perm,

USSR. Peshchery (Caves), 6-7, 33-39.

Munroe, J., Kimble, K., Spötl, C., Marks, G.S., McGee, D., Herron, D., 2021. Cryogenic cave carbonate and implications for thawing permafrost at Winter Wonderland Cave, Utah, USA. Scientific Reports, 11(1), 6430. <a href="https://doi.org/10.1038/s41598-021-85658-9">https://doi.org/10.1038/s41598-021-85658-9</a>

Povară, I., Diaconu, G., 1974. Déroulement du processus de gélifraction dans le milieu souterrain. Travaux de l'Institute de Spéologie "Emile Racovitza", 13, 139–146.

Richter, D., Riechelmann, D., 2008. Late Pleistocene cryogenic calcite spherolites from the Malachitdom Cave (NE Rhenish Slate Mountains, Germany): origin, unusual internal structure and stable C-O isotope composition. International Journal of Speleology, 37(2), 119–129.

### https://doi.org/10.5038/1827-806X.37.2.5

Richter, D.K., Meissner, P., Immenhauser, A., Schulte, U., Dorsten, I., 2010. Cryogenic and non-cryogenic pool calcites indicating permafrost and non-permafrost periods: a case study from the Herbstlabyrinth-Advent Cave system (Germany). The Cryosphere, 4(4), 501–509. https://doi.org/10.5194/tc-4-501-2010

Spötl, C., 2008. Kryogene Karbonate im Höhleneis der

Eisriesenwelt. Die Höhle, 59(1-4), 26-36.

Spötl, C., Koltai, G., Jarosch, A.H., Cheng, H., 2021. Increased autumn and winter precipitation during the Last Glacial Maximum in the European Alps. Nature Communications, 12(1), 1839.

https://doi.org/10.1038/s41467-021-22090-7

Teehera, K.B., Jungbluth, S.P., Onac, B.P., Acosta-Maeda, T.E., Hellebrand, E., et al., 2018. Cryogenic minerals in Hawaiian lava tubes: A geochemical and microbiological exploration. Geomicrobiology Journal, 35(3), 227–241.

https://doi.org/10.1080/01490451.2017.1362079

Žák, K., Hercman, H., Orvosova, M., Jackova, I., 2009. Cryogenic cave carbonates from the Cold Wind Cave, Nízke Tatry Mountains, Slovakia: Extending the age range of cryogenic cave carbonate formation to the Saalian. International Journal of Speleology, 38(2), 139–152.

https://doi.org/10.5038/1827-806X.38.2.5

Žák, K., Onac, B.P., Kadebskaya, O.I., Filippi, M., Dublyansky, Y., Luetscher, M., 2018. Cryogenic mineral formation in caves, In: Persoiu, A., Lauritzen, S.E. (Eds.), Ice caves. Elsevier, 123–162.

https://doi.org/10.1016/B978-0-12-811739-2.00035-8

Žák, K., Onac, B.P., Perşoiu, A., 2008. Cryogenic carbonates in cave environments: A review. Quaternary International, 187(1), 84–96.

https://doi.org/10.1016/j.quaint.2007.02.022

Žák, K., Richter, D.K., Filippi, M., Živor, R., Deininger, M., Mangini, A., Scholz, D., 2012. Coarsely crystalline cryogenic cave carbonate – a new archive to estimate the Last Glacial minimum permafrost depth in Central Europe. Climat of the Past, 8(6), 1821–1837.

https://doi.org/10.5194/cp-8-1821-2012

Žák, K., Urban, J., Cilek, V., Hercman, H., 2004. Cryogenic cave calcite from several Central European caves: age, carbon and oxygen isotopes and a genetic model. Chemical Geology, 206, 119–136.

https://doi.org/10.1016/j.chemgeo.2004.01.012